J. Fluid Mech. (2007), *vol.* 580, *pp.* 3–29.
doi:10.1017/S0022112007005320 Printed in the United Kingdom

On the thermal buffering of naturally ventilated buildings through internal thermal mass

J. M. HOLFORD AND A. W. WOODS
BP Institute, University of Cambridge, Cambridge CB3 0EZ, UK

(Received 21 October 2005 and in revised form 11 November 2006)

In this paper we examine the role of thermal mass in buffering the interior temperature of a naturally ventilated building from the diurnal fluctuations in the environment. First, we show that the effective thermal mass which is in good thermal contact with the air is limited by the diffusion distance into the thermal mass over one diurnal temperature cycle. We also show that this effective thermal mass may be modelled as an isothermal mass. Temperature fluctuations in the effective thermal mass are attenuated and phase-shifted from those of the interior air, and therefore heat is exchanged with the interior air. The evolution of the interior air temperature is then controlled by the relative magnitudes of (i) the time for the heat exchange between the effective thermal mass and the air; (ii) the time for the natural ventilation to replace the air in the space with air from the environment; and (iii) the period of the diurnal oscillations of the environment. Through analysis and numerical solution of the governing equations, we characterize a number of different limiting cases. If the ventilation rate is very small, then the thermal mass buffers the interior air temperature from fluctuations in the environment, creating a near-isothermal interior. If the ventilation rate increases, so that there are many air changes over the course of a day, but if there is little heat exchange between the thermal mass and interior air, then the interior air temperature locks on to the environment temperature. If there is rapid thermal equilibration of the thermal mass and interior air, and a high ventilation rate, then both the thermal mass and the interior air temperatures lock on to the environment temperature. However, in many buildings, the more usual case is that in which the time for thermal equilibration is comparable to the period of diurnal fluctuations, and in which ventilation rates are moderate. In this case, the fluctuations of the temperature of the thermal mass lag those of the interior air, which in turn lag those of the environment. We consider the implications of these results for the use of thermal mass in naturally ventilated buildings.

1. Introduction

A significant proportion of the world's energy is used to maintain a comfortable climate within buildings. International Energy Agency (2005) calculations suggest that in 1973, while industry and transport accounted for 42% and 25% respectively of the world's energy use, the agriculture, commercial, public sector and residential sectors contributed the remaining 33%. In the last three sectors listed, the maintenance of comfortable conditions within buildings accounts for a significant fraction of the energy use. From statistics for 2002 collected by the Department of Trade and Industry (2005) in the UK, it can be shown that space heating, cooling and ventilation in buildings in the service and domestic sectors accounted for 23% of the country's

primary energy use (44% of the 17% of energy used in the service sector and 50% of the 31% of energy used in the domestic sector: see tables 1.7, 3.8 and 5.6). Hence heating and cooling, combined with the mechanical distribution of air, in order to maintain a ventilated thermally comfortable interior, is energy-intensive.

An alternative low-energy solution is to use the diurnal variations in the environmental temperature to exchange heat with the exposed structure of a building, and, if possible, to drive this heat exchange with natural buoyancy-driven flow. If the structure of the building is cooled at night, the cooled material may be used during the day as a heat sink to regulate the interior heat loads, and hence the temperature, within the building. Alternatively, in cooler weather, heat from any daytime solar gain can be stored in the structure for release at night. Exposed building structure used in this manner is termed thermal mass. While floor coverings and lightweight ceiling panels can insulate the thermal mass from the interior, it is an established practice to leave some thermal mass exposed. In the Building Research Establishment's Low Energy Office, built in 1981, thermal mass was exposed in the interior ceiling in order to improve the thermal stability, as described in Crisp, Fisk & Salvidge (1984). Concrete floor slabs can be well-finished and left exposed in parts of some buildings, such as the Millennium Galleries in Sheffield, described in Long (2001). In larger buildings, incoming air can be routed through a plenum or undercroft of exposed concrete, as in the Lanchester Library, Coventry University, described in Cook, Lomas & Eppel (1999). As well as providing a reservoir of heat, heat may be transmitted through thermal mass adjacent to the environment, although modern building techniques are designed to minimize this transfer by incorporating an insulating layer within the structure. If there is no route for heat transmission to the environment, then the thermal mass is termed an internal thermal mass. The successful design of a thermally massive building requires accurate modelling of the heat balance in the interior.

The interior air temperature is affected by heating and ventilation. Occupied buildings must be ventilated to maintain a healthy interior environment, with low levels of carbon dioxide, dust and other pollutants. One method is by natural stack ventilation, allowing the difference in hydrostatic (stack) pressure to drive an exchange between the interior and the environment, as described by Linden, Lane-Serff & Smeed (1990) and Gladstone & Woods (2001). Even when local wind provides an alternative ventilation mechanism, the stack effect can still be important in thermally massive buildings, as in the Sri Lankan courtyard building studied by Rajapaksha, Nagai & Okumiya (2003). The steadiness of the stack pressure force over several hours may contribute to the importance of this mode of ventilation. Over the course of a diurnal cycle, the interior space may switch between being warmer than the environment to being cooler than the environment, causing the ventilation flow to change direction through the openings. The interior air can be heated by radiators, solar gain, occupants, electrical equipment, air-handling units and convective exchange with the building structure. (The last two sources may instead cool the interior air.) For most heating sources, the heat flux can be estimated or measured directly. However, for heat exchanged with the building structure, the heat flux depends on the temperature difference between the air and the structure surface, and hence on the temperature profile within the structure. A sketch of heat exchange driven by convection and ventilation in a space with internal thermal mass is shown in figure 1. The heat exchange in a building with external thermal mass is a more complex problem, as the penetration depths of temperature variations from the two sides both influence heat transfer, and may overlap. The model investigated here is a simpler case for an initial study.

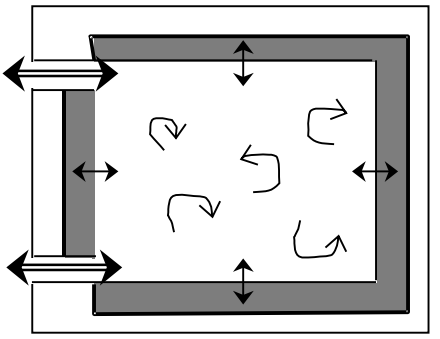

FIGURE 1. A sketch of a simple ventilated space with a well-mixed interior and internal thermal mass (shaded). Heat is transferred between the interior air and the thermal mass by convection, shown as the single solid arrows, and between the interior air and the environment by the ventilation flow, shown as the double solid arrows.

In general, the environment temperature varies approximately harmonically on the diurnal cycle, with moderate day-to-day variations as the weather changes. Therefore much work has focused on the response of a building to a harmonically varying environment temperature. Theoretical calculation of the interior temperature of a thermally massive building without ventilation, or with forced (constant flow rate) ventilation, is possible in many simplified cases. A number of examples are given in Pratt (1981). The large heat store provided by thermal mass attenuates the environmental variation, and introduces a phase lag, owing to the time taken for heat to diffuse into and out of the thermal mass. Both these features are useful in moderating interior conditions, as the peak interior temperature can be delayed beyond the period of use of the building.

Models of the heat balance in more realistic buildings are usually based on the 'conduction transfer function' (CTF) method or on the 'response factor' method. In the CTF method, linear relationships connect the Fourier components of the temperature and heat flux at the two surfaces of any thermal mass across which the heat flow is one-dimensional: see, for example, Fisk (1981). Then an exact analogy can be made between heat flow through a thermal mass and current flow through a trio of impedances in an electric circuit. In the 'RC method' these complex impedances are approximated, under limiting conditions, by a simpler network of resistances and capacitances. Internal thermal mass can be approximately incorporated in the RC method as a capacitance to ground, as in Lombard & Mathews (1999). Alternatively, in the response factor method (Stephenson & Mitalas 1967; Mitalas 1968), the temperature response of the structure to a heat pulse is summed to give the response to any heating time series. Approximations are introduced when these methods are applied to real buildings and, as a result, implementations give different results for test simulations, especially of thermally massive buildings, as shown by Bansal & Bhandari (1996).

At a single frequency, Li & Yam (2004) identified three parameters that control the dynamics of a diffusive internal thermal mass affected by forced ventilation. They showed that the phase lag of the interior temperature is at most $\pi/2$, and that the convective heat transfer number (ratio of convective to ventilation heat flux), the time constant (the time for ventilation to flush through an amount of air with the heat capacity of the thermal mass) and the penetration depth of the varying signal all affect the phase lag and attenuation. Major simplifications can be made if the thermal

mass can be modelled as a 'lumped mass', that is, assumed to be at a uniform temperature. Yam, Li & Zheng (2003) derived analytic expressions for the phase lag and attenuation in this situation.

The theoretical calculations for forced ventilation rely on the linear dependence of each heat flux on the temperature difference. Under natural ventilation, the flow rate itself varies, causing the ventilation heat flux to vary nonlinearly with the difference between the interior and environment temperature. Some numerical calculations for natural ventilation of an internal lumped thermal mass are given by Yam, Li & Zheng (2003), showing close-to-periodic variation of the interior temperature. Here, we build on this work, with a fundamental investigation of the thermal balance in a naturally ventilated space. We use a numerical solution for the full diffusion–convection–ventilation equations, and an approximate lumped model which we motivate from and compare with the full model. This establishes the range of parameters across which a lumped model may be accurately applied to model temperature fluctuations in a naturally ventilated building with internal thermal mass. We then explore the model in a number of idealized scenarios.

The paper is arranged as follows. In § 2, a full model for the heat balance in the interior of a naturally ventilated building with internal thermal mass is presented. Some preliminary scalings are used to identify the controlling parameters of the system, and several full numerical solutions illustrate the range of behaviour of the interior air and thermal mass temperatures. In the remainder of the paper, a simpler model, which is a generalized lumped mass model, is derived and compared with the full numerical solutions, and used to interpret the results. First, in § 3, the diffusion of heat into an internal thermal mass layer adjacent to air at a harmonically varying temperature is considered. The exact theoretical solution is calculated, and an equivalent lumped mass model is derived. Then, in § 4, the results of the analysis in § 3 are used to motivate a generalized lumped mass model which describes the thermal evolution of a naturally ventilated space subject to harmonic forcing of the environment temperature. The generalized lumped mass model predictions are compared with the numerical solutions of the full diffusive thermal mass model from § 2, for the case of a naturally ventilated building. The generalized lumped mass model is then studied in detail, and approximate solutions are derived in order to provide insight into the relative importance of heat transfer to the thermal mass and by ventilation in various parameter ranges. Conclusions are drawn in § 5.

2. Model of a naturally ventilated space with internal thermal mass

In this section a model to describe the response of a naturally ventilated space with internal thermal mass to harmonic variations in the environment temperature is presented and analysed. In order to derive insight into the principles of heat exchange in this building design, we focus on the situation in which internal heat loads are small and may be neglected. The interior air temperature is then determined by the balance between heat exchange with the thermal mass, and heat exchange with the environment through natural ventilation. Thermally massive buildings offer great potential for energy savings when the environment temperature is close to or above the human comfort temperature, but has wide diurnal variations, when internal heat loads can be small. In the alternative limit of large internal heat gains, the situation is simpler, as the high heat gains will drive a large ventilation flow. While the mean interior air temperature will be increased, the rapid flushing of the interior space will cause the variation in interior air temperature to follow the environment temperature variation

closely. A follow-up study will consider the response of a naturally ventilated space with internal thermal mass to a constant internal heat load of intermediate strength.

Modern building structures are complex, layered structures, in which each layer has different thermal properties, and layers are separated by interfaces or connections that may themselves introduce barriers to heat flow. However an internal thermal mass will typically be a layer of a single material, with known thermal properties. Heat is transferred away from the thermal mass into air by diffusion and convection. The heat flux can be measured by a heat transfer coefficient h, that is, the heat flux transferred per unit area, per degree difference in temperature ΔT between the thermal mass surface and the air far from the surface. The heat flux depends on (i) ΔT, (ii) whether a constant surface temperature or constant heat flux is maintained, (iii) the orientation of the surface and (iv) the air properties. A summary of many studies quantifying the heat flux is given in Gebhart *et al.* (1988), and is used in the following analysis.

Above a warm floor or below a cool ceiling, the heat transfer coefficient is a constant for small temperature differences, but increases as $\Delta T^{1/3}$ as turbulent convection develops. At the walls, a wall boundary layer flow develops, and the heat flux is introduced into the bulk of the interior air when the boundary layer flow fills the space from the floor or ceiling, as in the classic filling box model of Baines & Turner (1969). The transition to turbulence may occur part-way up a wall, leading to a temperature dependence of h in the range $\Delta T^{1/4}$ to $\Delta T^{1/3}$. Below a warm ceiling or above a cold floor, the heat transfer coefficient will depend sensitively on any mechanism that strips away the developing thermal boundary layer. Hence the heat transfer coefficient h increases with temperature difference, markedly so for horizontal surfaces, and has a different numerical value depending on the orientation of the surface. The aim of the present study is to consider a highly idealized problem, and quantify the accuracy of a simplified model of thermal mass under the nonlinear effects of natural ventilation. Therefore, within this model, it is assumed that the heat transfer coefficient takes a constant representative value.

Many components in a building, both of different structural elements and of items such as furniture within, can contribute to the exposed thermal mass of the space. Here, all internal thermal mass is assumed to be evenly distributed around the walls, floor and ceiling, in a simplified model chosen to allow development of theoretical understanding. It is expected that this model will be most applicable to the situation where there is one dominant element of thermal mass, as is often the case in buildings which have been designed to be heavyweight. Further work would be needed to understand the interaction of different elements of internal thermal mass. While temperature gradients in the interior air can occur, due to the spatial distribution of ventilation openings and heat sources, it is assumed here that the space remains well mixed. Radiative transfers within a space can be significant, and act to bring all surface temperatures into equilibrium. For evenly distributed thermal mass surrounding a well-mixed space, the thermal mass surface is *a priori* isothermal and radiation can be neglected. The effects of corners will also be neglected, so that the diffusion of heat into the thermal mass depends only on x, the distance from the back of the thermal mass.

The thermal mass can then be modelled by a layer of material with thermal diffusivity κ, density ρ and specific heat capacity c, occupying $0 < x < l$, in contact with the interior air at temperature T_i at $x = l$, and insulated at $x = 0$, as sketched in figure 2. The temperature within the layer $T(x, t)$ then evolves with time t as

$$\frac{\partial T}{\partial t} = \kappa \frac{\partial^2 T}{\partial x^2}, \tag{2.1}$$

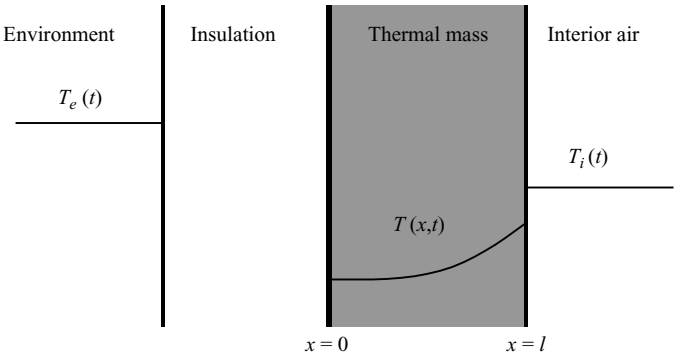

FIGURE 2. A sketch of the one-dimensional representation of an internal thermal mass adjacent to a well-mixed interior, showing typical instantaneous environment, thermal mass and interior air temperatures.

subject to the boundary conditions

$$\left.\frac{\partial T}{\partial x}\right|_{x=0} = 0, \quad \kappa\rho c \left.\frac{\partial T}{\partial x}\right|_{x=l} = h[T_i - T|_{x=l}]. \tag{2.2}$$

A harmonic variation in the environment temperature T_e, of the form

$$T_e(t) = T_0 + \Delta T \cos(\omega t) = T_0 + \mathrm{Re}[\Delta T \mathrm{e}^{\mathrm{i}\omega t}], \tag{2.3}$$

is imposed. If ventilation occurs through openings separated by a height H with a combined effective area of A^*, the ventilation flow rate q is given by

$$q = A^* \sqrt{\alpha g H |T_e - T_i|}, \tag{2.4}$$

where α is the coefficient of thermal expansion and g is the acceleration due to gravity. Then the interior temperature evolves as

$$\rho_i V_i c_i \frac{\mathrm{d}T_i}{\mathrm{d}t} = Sh(T|_{x=l} - T_i) + \rho_i c_i A^* (T_e - T_i) |\alpha g H (T_e - T_i)|^{1/2}, \tag{2.5}$$

where V_i, ρ_i and c_i are the volume, density and specific heat capacity of the air within the interior space and S is the surface area of the thermal mass exposed to the interior air.

It is convenient to work with dimensionless variables. The forcing is provided by the environment temperature variation, suggesting $t_1 = 1/\omega$ as the reference time scale and ΔT as the reference temperature scale. We define the dimensionless time, temperature and position within the thermal mass to be $\tau = \omega t$, $\theta = (T - T_0)/\Delta T$ and $X = x/l$, respectively. Then, from (2.1)–(2.3) and (2.5), the dimensionless environment temperature is $\theta_e(\tau) = \mathrm{e}^{\mathrm{i}\tau}$ and the dimensionless temperature within the thermal mass $\theta(X, \tau)$ evolves as

$$\frac{\partial \theta}{\partial \tau} = \frac{1}{2\eta^2} \frac{\partial^2 \theta}{\partial X^2}, \tag{2.6}$$

where $\eta = l\sqrt{\omega/2\kappa}$, subject to the boundary conditions

$$\left.\frac{\partial \theta}{\partial X}\right|_{X=0} = 0, \quad \left.\frac{\partial \theta}{\partial X}\right|_{X=1} = \frac{2\eta^2}{\xi}(\theta_i - \theta|_{X=1}), \tag{2.7}$$

Time scale	Time scale for	Expression	Value for construction type: light	moderate	heavy
t_1	forcing	$\frac{1}{\omega}$	3.8 hr	3.8 hr	3.8 hr
t_2	convection to affect mass temperature	$\frac{l\rho c}{h}$	1.5 hr	6.7 hr	26 hr
t_3	diffusion to affect mass temperature	$\frac{l^2}{\kappa}$	0.23 hr	8.8 hr	3.9 hr
t_4	ventilation to affect interior temperature	$\frac{V_i}{q_0}$	0.13 hr	0.13 hr	0.13 hr
t_5	convection to affect interior temperature	$\frac{\rho_i c_i V_i}{hS}$	0.17 hr	0.17 hr	0.17 hr

TABLE 1. Time scales for various heat transfer processes in a building, with values for three construction types. Note the ventilation rate scale $q_0 = A^*\sqrt{\alpha g H \Delta T}$.

where $\xi = \omega\rho c l/h$. Finally, the dimensionless interior temperature evolves as

$$\epsilon \frac{\mathrm{d}\theta_i}{\mathrm{d}\tau} = \frac{1}{\xi}(\theta|_{X=1} - \theta_i) + \epsilon R_n(\theta_e - \theta_i)|\theta_e - \theta_i|^{1/2}, \tag{2.8}$$

where $R_n = A^*\sqrt{\alpha g H \Delta T}/V_i\omega$ and $\epsilon = V_i\rho_i c_i/Sl\rho c$. Integrating (2.6) over the thickness of the thermal mass, using boundary conditions (2.7), gives

$$\frac{\partial\theta}{\partial\tau} = \frac{1}{2\eta^2}\frac{\partial^2\theta}{\partial X^2}, \tag{2.6}$$

where $\eta = l\sqrt{\omega/2\kappa}$, subject to the boundary conditions

$$\left.\frac{\partial\theta}{\partial X}\right|_{X=0} = 0, \quad \left.\frac{\partial\theta}{\partial X}\right|_{X=1} = \frac{2\eta^2}{\xi}(\theta_i - \theta|_{X=1}), \tag{2.7}$$

$$\frac{\mathrm{d}\theta_{mean}}{\mathrm{d}\tau} = \frac{1}{\xi}(\theta_i - \theta|_{X=1}), \tag{2.9}$$

in terms of the mean thermal mass temperature $\theta_{mean} = \int_0^1 \theta|_X \,\mathrm{d}X$.

The four non-dimensional parameters η, ξ, R_n and ϵ that appear during the non-dimensionalization can be interpreted in terms of the time scales for temperature changes caused by various processes in the space, shown in table 1. The two processes that control the heat transfer from the thermal mass are convection at the surface (on a time scale $t_2 = l\rho c/h$) and diffusion within the thermal mass (on a time scale $t_3 = l^2/\kappa$). The ratio $2\eta^2 = l^2\omega/\kappa = t_3/t_1$ of the time scale for diffusion to the forcing time scale, appearing in (2.6), indicates whether there is time for temperature variations to penetrate the thermal mass before the environment temperature changes appreciably. The parameter η represents the ratio of the layer thickness l to the penetration depth $\delta = \sqrt{2\kappa/\omega}$ of temperature variations into the thermal mass. Hence there is an effective thermal mass, of thickness $\min(\delta, l)$, which represents that part of the thermal mass whose temperature varies over the period of diurnal fluctuations. The ratio $\xi = \omega\rho c l/h = t_2/t_1$ of the time scale for convection to the forcing time scale, appearing in (2.7), indicates whether there is time for significant heat to be transferred to the thermal mass before the environment temperature changes appreciably. For $\eta > 1$, we expect ξ/η to represent the degree of thermal equilibration between the interior air and the effective thermal mass.†

† In related work on steady heat transfer, the Biot number $\mathscr{L} = 2\eta^2/\xi = t_3/t_2$ is often used to indicate whether convection at the surface of the thermal mass ($\mathscr{L} \ll 1$) or diffusion within the thermal mass ($\mathscr{L} \gg 1$) limits heat transfer. The values in table 1 suggest that convection is commonly the limiting process.

The parameters ξ and η control the heat exchange with the thermal mass, independently of the degree or type of ventilation. In order to estimate the time scale for heat transfer by ventilation, a scale for the interior/environment temperature difference is needed. Choosing the amplitude of environmental temperature variations ΔT, the typical ventilation rate is $q_0 = A^* \sqrt{\alpha g H \Delta T}$, giving the time for ventilation to affect the interior temperature as $t_4 = V_i/q_0$. This time scale is the analogue of the flushing time scale defined by Holford & Hunt (2000) (for a well-mixed space, with the temperature difference scale set by the initial conditions) or Kaye & Hunt (2004) (for a two-layer stratification, with the temperature difference scale set by plume dynamics). In both these earlier studies, the competition between a flushing time scale and a heating (Holford & Hunt 2000) or filling (Kaye & Hunt 2004) time scale was used to understand the dynamics of natural ventilation in an insulated space. In the current work, there is no simple heating time scale because of the complexity of heat transfer from the thermal mass. Our third non-dimensional parameter is the ratio of the forcing time scale to the time to flush the interior space, $R_n = q_0/V_i\omega = t_1/t_4$.

Convection affects the temperatures of the thermal mass and interior air on time scales of t_2 and t_5, respectively. The fourth parameter $\epsilon = V_i\rho_i c_i/Sl\rho c = t_5/t_2$ is the ratio of the heat capacity of the interior air to the heat capacity of the thermal mass. In studies of forced ventilation, the dimensional time constant $t_c = \rho c l S/\rho_i c_i q_f$ is a commonly used parameter. It is the time for ventilation at a volume flow rate q_f between spaces at a temperature difference ΔT to bring in an amount of heat equal to that that would be stored in the thermal mass by raising its temperature by ΔT. Based on the typical ventilation rate q_0, $t_c = t_2 t_4/t_5 = t_1/\epsilon R_n$.

In order to calculate the range of appropriate values of the time scales and parameters in this model, three typical construction materials (light, moderate and heavy) from the guide by the Chartered Institution of Building Services Engineers, CIBSE (1999), will be considered. Values for the time scales t_1 to t_5 are given in table 1. For simplicity the dominant contribution is assumed to come from the walls, as would be the case with a carpet floor finish, and a false ceiling. We shall assume perfect insulation and consider the internal thermal mass of the inner leaf of construction, neglecting the contribution of surface plaster finishes. The standard constant convective heat transfer coefficient for walls from table 3.8 from CIBSE (1999) is $h = 2.5\ \mathrm{W\,m^{-2}\,K^{-1}}$. Values will be calculated for a generic single space with square floor area, of height $H = 2.5\,\mathrm{m}$, volume $V_i = 60\ \mathrm{m^3}$ and thermal mass surface area $S = 49\ \mathrm{m^2}$, with a total effective ventilation opening area of $A^* = 0.2\ \mathrm{m^2}$, and for an amplitude of environmental temperature variations of $\Delta T = 5\,\mathrm{K}$. The typical ventilation rate is then $q_0 = 0.13\ \mathrm{m^3\,s^{-1}}$, showing that the space can be flushed many times over the diurnal cycle ($R_n = 30$).

In lightweight buildings with timber frame walls a common interior surface is 13 mm plasterboard (CIBSE 1999, table 3.54, 10). This thin, lightweight material behaves as a lumped mass ($\eta = 0.03$) and is rapidly affected by diurnal temperature variations ($\xi = 0.40$), while having a thermal capacity of only ten times the interior air ($\epsilon = 0.10$). A more substantial alternative is a cavity wall construction, with 100 mm lightweight aggregate concrete blocks as the inner leaf (CIBSE 1999, table 3.54, 8). This thicker material no longer behaves as a lumped thermal mass ($\eta = 1.07$) and is slow to respond to diurnal changes ($\xi = 1.8$), with a thermal capacity many times that of the interior air ($\epsilon = 0.025$). If instead the inner leaf of the cavity is constructed from 100 mm dense concrete blocks (CIBSE 1999, table 3.54, 7), then temperature variations penetrate the blocks more fully ($\eta = 0.72$), due to the higher

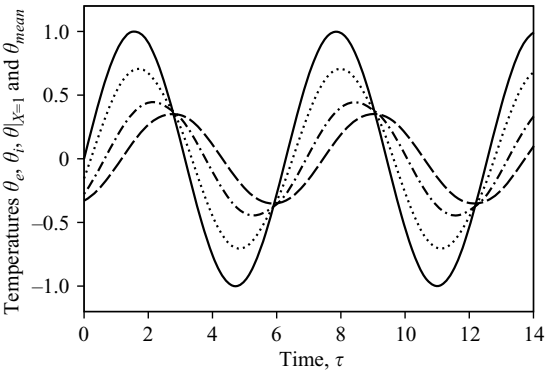

FIGURE 3. Time series of the temperature in the environment θ_e (solid), interior θ_i (dotted), thermal mass surface $\theta|_{X=1}$ (dot-dashed) and thermal mass mean θ_{mean} (dashed), from numerical integration of the full diffusion model with $\eta = 1$, $\xi = 1$ and $F_n = 2$.

thermal diffusivity. However, the greater thermal capacity of the blocks causes the temperature of the mass to change much more slowly ($\xi = 6.7$), and increases the thermal capacity relative to that of the air many fold ($\epsilon = 0.0065$).

In all but very lightweight buildings, many volumes of interior air must be flushed through the space before an amount of heat comparable to that in the thermal mass is brought in, because $\epsilon \ll 1$. Therefore, on all but the shortest time scales, the heat capacity of the air can be neglected, and the interior temperature assumed to adjust instantaneously to balance the fluxes of heat into the interior. The strength of the ventilation may now be expressed as the ratio of ventilation to convective heat fluxes,

$$F_n = \rho_i c_i q_0 / Sh = \epsilon \xi R_n = t_5 / t_4, \tag{2.10}$$

which is $O(1)$ in all three examples above. In the limit of small ϵ, (2.8) becomes

$$0 = \theta|_{X=1} - \theta_i + F_n(\theta_e - \theta_i)|\theta_e - \theta_i|^{1/2}. \tag{2.11}$$

A numerical integration of (2.6), (2.7) and (2.11), using the Crank–Nicholson method (see Press *et al.* 1989) is used to solve an initial value problem, continuing until the long-time solution is reached. Typical time series over several days are shown in figure 3, for the environment, interior air, thermal mass surface and mean thermal mass temperatures. The thermal mass and interior air temperatures approximate a harmonic variation, and can usefully be characterized by their phase lag and attenuation, with respect to the environment temperature. Here the phase lag is defined as the mean time delay of temperature variation extrema from the environment temperature extrema, and the attenuation is defined as the ratio of the peak-to-peak temperature variation in the environment to that of the variable. As expected, the environment variations are substantially attenuated in the mean temperature of the thermal mass, and have a significant phase lag. However, the attenuation and phase lag of the surface temperature of the thermal mass are not so marked. The interior temperature always lies between that of the environment and that of the thermal mass surface. There is no heat flux into the thermal mass at the time when the interior air and surface temperatures are equal (and equal to the environment, by (2.11)). Therefore the mean thermal mass temperature reaches its extrema at this time, from (2.9).

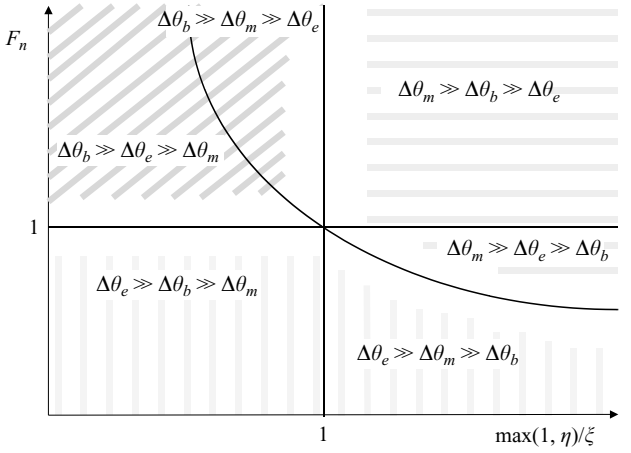

FIGURE 4. Range of behaviour for $F_n \gg 1$ or $F_n \ll 1$ and $\max(1, \eta)/\xi \gg 1$ or $\max(1, \eta)/\xi \ll 1$, from the scaling derived in the limits $\eta \gg 1$ and $\eta \ll 1$.

The influence of the parameters η, ξ and F_n can be estimated from a scaling analysis. Suppose that typical temperature scales are $\theta|_{X=1} \sim \Delta\theta_m$, $\theta_i - \theta|_{X=1} \sim \Delta\theta_b$ and $\theta_i - \theta_e \sim \Delta\theta_e$. Then in the limit $\eta \gg 1$, the temperature gradient within the thermal mass is concentrated in a surface layer of thickness $1/\eta$, while away from the surface layer the temperature variation is zero. The surface boundary condition (2.7) and the interior heat balance (2.11) imply that

$$\Delta\theta_m \sim \frac{\eta}{\xi}\Delta\theta_b, \quad \Delta\theta_b \sim F_n \Delta\theta_e^{3/2}. \tag{2.12}$$

Alternatively, in the limit $\eta \ll 1$, the thermal mass is approximately isothermal, at temperature θ_{mean}, and (2.6) may be replaced with

$$\frac{\mathrm{d}\theta_{mean}}{\mathrm{d}\tau} \approx \frac{1}{\xi}(\theta_i - \theta_{mean}), \tag{2.13}$$

which, with (2.11), gives

$$\Delta\theta_m \sim \frac{1}{\xi}\Delta\theta_b, \quad \Delta\theta_b \sim F_n \Delta\theta_e^{3/2}. \tag{2.14}$$

Hence $\max(1, \eta)/\xi$ and F_n are the controlling parameters for $\eta \gg 1$ and $\eta \ll 1$. When these two parameters are either large or small with respect to one, six possible orderings of the magnitude of the three temperature scales are possible, in the regions delineated in figure 4.

The attenuation of the mean thermal mass and interior air temperatures, denoted by A_{mean} and A_i respectively, can be estimated from

$$A_{mean} \sim \frac{\max(1, \eta)}{\Delta\theta_m}, \quad A_i \sim \frac{1}{1 - \Delta\theta_e}. \tag{2.15}$$

Neglecting any phase shift in temperature, the three temperature scales must approximately sum to one. Hence there are three distinctive limiting regimes, shown by the hatching in figure 4.

Regime I: $Fn \ll \min(1, \xi, \xi/\eta)$ (vertical hatching), when the largest temperature jump is between the interior air and the environment, with $\Delta\theta_e \sim 1$ and $\Delta\theta_m \sim$

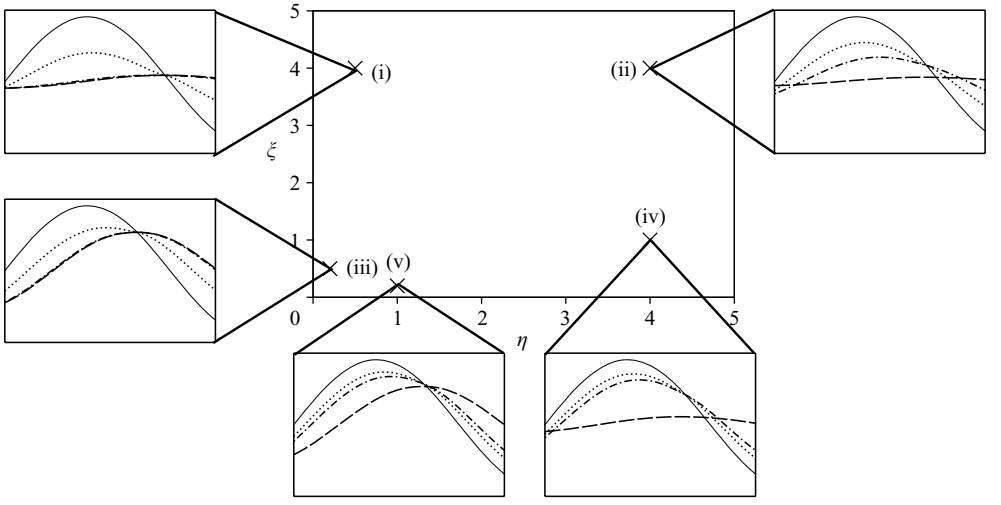

FIGURE 5. Variation across $\eta\xi$ parameter space of time series of the temperature in the environment θ_e (solid), interior θ_i (dotted), thermal mass surface $\theta|_{X=1}$ (dot-dashed) and thermal mass mean θ_{mean} (dashed), from numerical integration of the full diffusion model with $F_n = 1$. The parameters (η, ξ) are (i) (0.5, 4.0), (ii) (4.0, 4.0), (iii) (0.2, 0.5), (iv) (4.0, 1.0) and (v) (1.0, 0.2).

$\max(1, \eta)F_n/\xi$. The heat flux from ventilation is sufficiently small compared to that from the thermal mass that little temperature variation penetrates the building, and the attenuation of variations in the thermal mass and in the interior air are large, with $A_{mean} \sim \xi/F_n$ and $A_i \sim \infty$. Provided that ϵ is small enough to give adequate ventilation for air quality at this small F_n, this is the ideal regime for attenuating environmental variations.

Regime II: $\xi \ll \min(1, F_n)\max(1, \eta)$ (horizontal hatching), when the largest temperature jump is within the thermal mass, with $\Delta\theta_e \sim [\xi \min(1, 1/\eta)/F_n]^{2/3}$ and $\Delta\theta_m \sim 1$. There is significant opportunity for ventilation, combined with strong convection, so that both the interior air and thermal mass temperatures follow the environment closely, with $A_{mean} \sim \max(1, \eta)$ and $A_i \sim 1$. In this regime, there is no benefit from the thermal mass, as it cannot be maintained at a temperature different from the environment.

Regime III: $Fn \gg 1$ and $\xi \gg \max(1, \eta)$ (diagonal hatching), when the largest temperature jump is across the boundary layer adjacent to the thermal mass, with $\Delta\theta_e \sim 1/F_n^{2/3}$ and $\Delta\theta_m \sim \max(1, \eta)/\xi$. Once again there is significant opportunity for ventilation, but now combined with weak convection. The interior air and thermal mass temperatures diverge, with a large attenuation in the thermal mass of $A_{mean} \sim \xi$, but little attenuation in the interior air of $A_i \sim 1 + F_n^{-2/3}$. In this regime, interior conditions may benefit from an equable radiant temperature from the surface of the thermal mass, although the air temperature is little different from the environment.

A typical cross-section of behaviour as the thermal mass parameters η and ξ vary is shown for the parameter choice $F_n = 1$, in the time series clips in figure 5. The interior air and thermal mass surface temperatures converge as the parameter combination $\max(1, \eta)/\xi$ increases, from case (i) to case (v). In addition, for a convection time scale much longer than the forcing time scale ($\xi \gg 1$), the temperature changes within the thermal mass are small, as little heat can be fluxed in or out. For a thin thermal mass

layer ($\eta \ll 1$), the thermal mass temperature is uniform, as diffusion removes spatial variations more quickly than the forcing time scale. For a thicker layer ($\eta \geqslant 1$), temperature fluctuations are concentrated at the surface. In the remainder of this work, we develop a model which can be used to predict the phase lag and attenuation of temperature variations in the interior air and thermal mass.

3. The use of lumped models for internal thermal mass

It is desirable to investigate the dependence of the heat transfer between the interior air and the thermal mass on the parameters η and ξ. In particular, it is useful to know when the effects of thermal mass can be modelled by a lumped mass, that is, a mass at uniform temperature. In the previous section, approximately harmonic variations in the building temperatures were found from numerical solution of the full diffusion equations in the thermal mass, coupled with natural ventilation. Therefore, as a starting point for the analysis, we investigate the response of a thermal mass to a harmonically varying interior temperature $\theta_i(\tau) = \overline{\theta}_i e^{i\tau}$. If ventilation is forced at a constant flow rate, then a harmonic variation in the environment results in a harmonic variation in the interior.

As heat diffuses into the thermal mass, the temperature within the thermal mass takes the simple form $\theta(X, \tau) = \overline{\theta}(X)e^{i\tau} = \overline{\theta}_i e^{i(\tau-\phi(X))}/A(X)$, where the phase lag ϕ and attenuation A are real. From (2.6) and (2.7), the complex amplitude $\overline{\theta}(X)$ is given by

$$\overline{\theta}(X) = 2C\overline{\theta}_i \cos\eta X \cosh\eta X(1 + i\tan\eta X \tanh\eta X), \tag{3.1}$$

where

$$C = \frac{\eta}{\cos\eta\cosh\eta[2\eta + \xi(\tanh\eta - \tan\eta) + i\{2\eta\tan\eta\tanh\eta + \xi(\tanh\eta + \tan\eta)\}]}. \tag{3.2}$$

Hence the amplitude of the temperature variation at the exposed surface is

$$\overline{\theta}(1) = 2C\overline{\theta}_i \cos\eta\cosh\eta(1 + i\tan\eta\tanh\eta) = \frac{\overline{\theta}_i e^{-i\phi(1)}}{A(1)}, \tag{3.3}$$

and the mean thermal mass temperature is

$$\overline{\theta}_{mean} = \frac{C\overline{\theta}_i}{\eta}\cos\eta\cosh\eta[\tanh\eta + \tan\eta + i(\tan\eta - \tanh\eta)] = \frac{\overline{\theta}_i e^{-i\phi_{mean}}}{A_{mean}}. \tag{3.4}$$

Figure 6 shows typical profiles of the temperature within the thermal mass over one forcing period. The temperature varies within an envelope $\overline{\theta}_i/A(X)$ which decreases from the surface to the insulated boundary, while the phase lag $\phi(X)$ from the interior air temperature increases with distance from the surface. The relative attenuation and phase lag of temperature within the thermal mass vary with η, but do not depend on ξ. As ξ increases, and the effect of convection decreases, the attenuation and phase lag at the surface increase. For a thin layer of thermal mass ($\eta \ll 1$), the temperature of the thermal mass is close to uniform, as the penetration depth is larger than the layer thickness, while the surface temperature lags the environment temperature by $\tan^{-1}(\xi)$ and is attenuated by a factor $\sqrt{1+\xi^2}$.

A generalized lumped mass model is now derived, for this case of a harmonic interior air temperature variation. Equation (2.9) reveals that changes in the mean thermal mass temperature are due to temperature differences between the thermal mass surface and the interior air. In this lumped model we relate the thermal mass

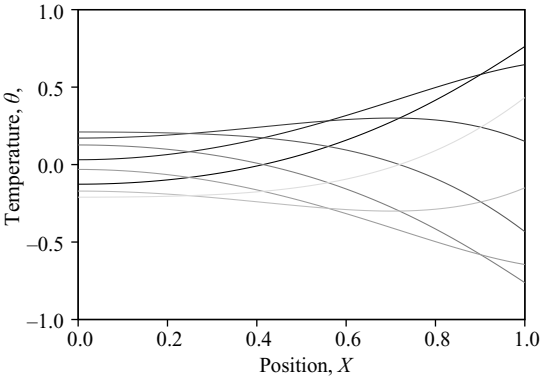

FIGURE 6. Eight temperature profiles (dark → light) in one period, at times $\tau = 0, \pi/4, \ldots, 7\pi/4$, across a thermal mass layer for which $\eta = 2$, $\xi = 1$, adjacent to interior air at temperature $\theta_i(\tau) = \cos(\tau)$.

surface temperature to the mean thermal mass temperature, which has a larger attenuation and phase lag. Writing

$$\frac{\mathrm{d}\theta_{mean}}{\mathrm{d}\tau} = \frac{1}{\xi}(\theta_i - \theta|_{X=1}) = \frac{\lambda}{\xi}\left(\theta_i - \frac{\theta_{mean}}{l_r}\right), \tag{3.5}$$

and requiring λ to be independent of time, l_r is chosen to be

$$l_r = \frac{1}{1 - \dfrac{\tan\phi_{mean}}{\tan\phi(1)}\left[1 - \dfrac{A(1)}{\cos\phi(1)}\right]} = \frac{(\cosh 2\eta - \cos 2\eta)}{\eta(\sinh 2\eta + \sin 2\eta)}, \tag{3.6}$$

and λ then takes the value

$$\lambda = 1 - \frac{\cos\phi(1)}{A(1)}\left[1 - \frac{\tan\phi(1)}{\tan\phi_{mean}}\right] = \frac{1}{1 + \dfrac{\eta(\sinh 2\eta - \sin 2\eta)}{\xi(\cosh 2\eta - \cos 2\eta)}}. \tag{3.7}$$

A bulk thermal mass temperature $\theta_m = \theta_{mean}/l_r$ can then be defined, which satisfies

$$\frac{\mathrm{d}\theta_m}{\mathrm{d}\tau} = \frac{1}{\Omega_L}(\theta_i - \theta_m), \tag{3.8}$$

where

$$\Omega_L = \frac{\xi l_r}{\lambda}. \tag{3.9}$$

The parameter Ω_L controls the heat exchange between the interior air and the thermal mass. For $\Omega_L \ll 1$, the effective thermal mass is in good thermal contact with the interior air and the bulk thermal mass temperature is similar to that of the interior air. For $\Omega_L \gg 1$, the effective thermal mass is in poor thermal contact with the interior air and the variation of the bulk thermal mass temperature is small. The inverse $1/\Omega_L$ may be interpreted as the degree of thermal equilibration between the effective thermal mass and the interior air, over the time scale of fluctuations in the temperature of the interior air.

The generalized lumped mass model can also be derived by physical reasoning, as follows. From consideration of the meaning of the parameter η, we assume that only some fraction l_r of the thermal mass layer responds to the temperature changes,

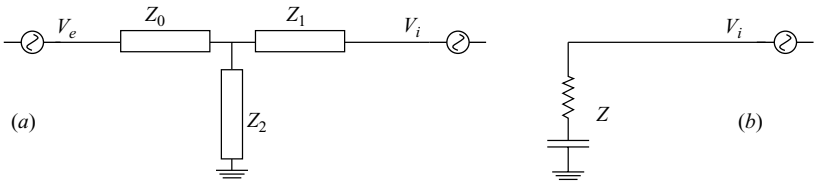

FIGURE 7. Electric circuits supporting a current analogous to periodic heat flow through a thermal mass, as in the CTF method. (*a*) Thermal mass connected to environment 'voltage' V_e and interior 'voltage' V_i is equivalent to a network of three complex impedances, Z_0, Z_1 and Z_2. (*b*) For an internal thermal mass, $Z_0 \to \infty$, $Z_1 = 0$ and $Z_2 = Z$ from (3.14).

and is at a uniform temperature θ_m. Also, we assume that the convective heat flux is proportional to the departure of some surface temperature θ_s from the interior temperature, where θ_s may be different from θ_m according to the relation

$$\theta_s = \lambda\theta_m + (1-\lambda)\theta_i, \tag{3.10}$$

for some λ. Dimensionally, the convective heat flux per unit area is $h(u_s - u_i) = h\lambda(u_m - u_i)$, and hence λ alters the effective heat transfer coefficient. It now follows that θ_m satisfies (3.8). The surface thermal mass and bulk thermal mass temperatures are also harmonic, $\theta_s(\tau) = \overline{\theta}_s e^{i\tau}$ and $\theta_m(\tau) = \overline{\theta}_m e^{i\tau}$, and the complex amplitudes of the thermal mass bulk and surface temperature variations are

$$\overline{\theta}_m = \frac{\overline{\theta}_i}{(1 + i\Omega_L)} \tag{3.11}$$

and

$$\overline{\theta}_s = \frac{[1 + i\Omega_L(1-\lambda)]}{(1 + i\Omega_L)}\overline{\theta}_i. \tag{3.12}$$

The surface temperature can be matched exactly between the full diffusive model (3.3) and the generalized lumped model (3.12) to give expressions for the effective thickness l_r and effective heat transfer coefficient λ as before. The parameter Ω_L is now seen to be the ratio of the time scale $\rho c l l_r/\lambda h$ for changes to the (thinner) lumped mass temperature by (reduced) convection, compared to the forcing time scale $1/\omega$.

Alternatively, the generalized lumped model can be derived within the framework of the CTF method. The one-dimensional flow of heat through a layer of thermal mass exposed at either side to air with harmonic temperature variations is analogous to the flow of electric current through a network of three complex impedances connected between two ac voltage supplies, shown in figure 7(*a*); see, for example, Fisk (1981). From the thermal mass surface temperature (3.3), it can be shown that the internal thermal mass, together with the convection at the surface, is equivalent to a dimensional impedance to ground in the CTF method of

$$Z = \frac{1}{h} + \frac{l}{\kappa\rho c(1+i)\eta \tanh[(1+i)\eta]}. \tag{3.13}$$

This impedance may be expressed as

$$Z = \frac{1}{\lambda h} + \frac{l}{i\omega\rho c l l_r}, \tag{3.14}$$

where the effective thickness l_r and effective heat transfer coefficient λ are as before. The first term is the impedance of a pure resistor, representing the process of

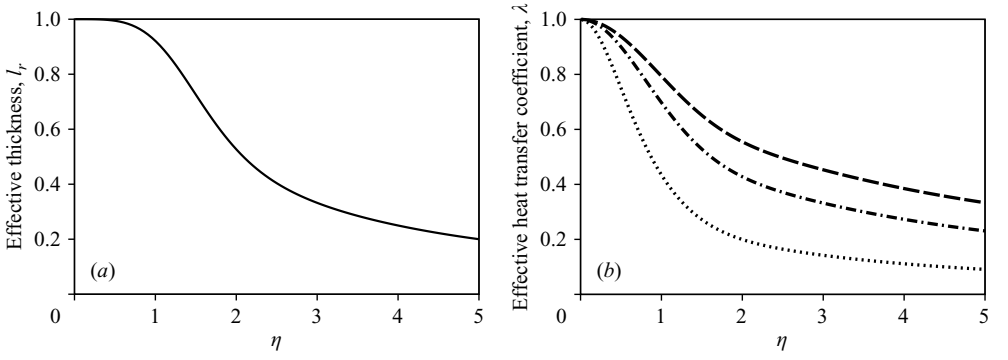

FIGURE 8. Generalized lumped model parameters as functions of η: (*a*) effective thickness l_r, and (*b*) effective heat transfer coefficient λ for $\xi = 0.5$ (dotted), 1.5 (dot-dashed) and 2.5 (dashed).

convection at the thermal mass surface, while the second term is the impedance of a pure capacitor, representing the heat storage capacity of a lumped thermal mass. Hence heat flow into an internal thermal mass is analogous to current flow in the circuit shown in figure 7(*b*).

The effective thickness l_r of the thermal mass is shown in figure 8(*a*). It is independent of ξ, satisfies $0 < l_r \leqslant 1$, is close to one for $\eta \ll 1$ and falls off as $1/\eta$ for $\eta \gg 1$. Therefore the dimensional effective thickness of the thermal mass, which equals the full thickness l for η small, is reduced to the penetration depth $\delta = \sqrt{2\kappa/\omega}$ for η large. The effective heat transfer coefficient λ is shown in figure 8(*b*) for three values of ξ, and decreases as ξ decreases. It also satisfies $0 < \lambda \leqslant 1$, is close to one for $\eta \ll \max(\xi^{1/2}, \xi)$ and falls off as ξ/η for $\eta \gg \max(1, \xi)$. Therefore the dimensional heat transfer coefficient, which is the true coefficient h for η small compared to ξ, is reduced to $\omega\rho c\delta$, the amount of heat stored per unit area in the thermal mass within one penetration depth of the surface, for η large compared to ξ. In the latter limit, convection is strong enough to carry heat away from the thermal mass at a greater rate than diffusion can maintain the temperature of the surface layer.

The parameter Ω_L can be written

$$\Omega_L = \frac{\xi(\cosh 2\eta - \cos 2\eta) + \eta(\sinh 2\eta - \sin 2\eta)}{\eta(\sinh 2\eta + \sin 2\eta)}. \tag{3.15}$$

This takes the value $\Omega_l \sim \xi$ for $\eta \ll \min(1, \xi)$ and falls off as $\Omega_L \sim 1 + \xi/\eta$ for $\eta \gg 1$. Hence $1/\Omega_L$ is the more exact counterpart of the parameter combination $\max(1, \eta)/\xi$, identified in the scaling analysis of § 2 as indicative of the role of the thermal mass. For the three types of building construction considered in table 1, $\Omega_L = 0.4$, 2.3 and 6.9, for the lightest to heaviest construction types, respectively.

In terms of the attenuation and phase lag, if the interior temperature is given by $\theta_i(\tau) = \cos(\tau - \phi_i)/A_i$, then the bulk temperature is $\theta_m(\tau) = \cos(\tau - \phi_m)/A_m$, where

$$\frac{A_i}{A_m} = \frac{1}{\sqrt{1 + \Omega_L^2}} \tag{3.16}$$

and

$$\tan(\phi_m - \phi_i) = \Omega_L. \tag{3.17}$$

Note that the thermal mass reaches an extremum of temperature when the bulk thermal mass and interior air temperatures are equal, as $\theta_m(\phi_m) = 1/A_m =$

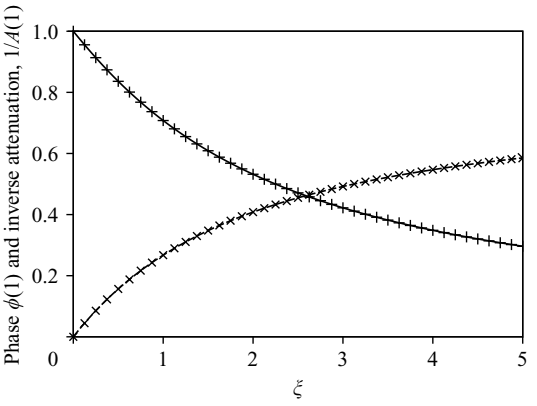

FIGURE 9. Comparison of the variation with ξ of the phase lag ($\times$ and dashed line) and inverse attenuation ($+$ and solid line) of the thermal mass surface temperature with respect to the interior air temperature at $\eta = 1.5$ between the full diffusion solution (symbols) and the generalized lumped model (lines).

$\cos(\phi_m - \phi_i)/A_i = \theta_i(\phi_m)$. The attenuation A_{mean} of the mean thermal mass temperature θ_{mean} is greater than the attenuation A_m of the bulk thermal mass temperature, as $A_{mean} = A_m/l_r$. The temperature of the exposed thermal mass surface is given by the intermediate temperature $\theta_s(\tau) = \cos(\tau - \phi_s)/A_s$, where

$$\frac{A_s}{A_m} = \frac{1}{\sqrt{1 + \Omega_L^2(1-\lambda)^2}} \tag{3.18}$$

and

$$\tan(\phi_m - \phi_s) = (1-\lambda)\Omega_L. \tag{3.19}$$

The predictions of this generalized lumped model are compared with those of the full model, accounting for diffusive heat transfer within the thermal mass under forced ventilation in figure 9, for one value of η. As ξ increases, the relative phase lag $\phi(1) = \phi_s - \phi_i$ and attenuation $A(1) = A_s/A_i$ of the surface temperature increase.

The parameters Ω_L and λ are related by

$$(1-\lambda)\Omega_L = \frac{\sinh 2\eta - \sin 2\eta}{\sinh 2\eta + \sin 2\eta}. \tag{3.20}$$

Therefore, from (3.18)–(3.20), the relationship between the surface and bulk thermal mass temperatures depends only on η. For η small, the whole depth of the thermal mass is affected by variations, and so the bulk and surface thermal mass temperatures are similar. For η large, only the surface of the thermal mass is affected by variations, and so the bulk temperature variations are weaker and lag by $\pi/4$.

The variation of Ω_L and λ with η and ξ is shown in figure 10. This can be compared with the time series clips in figure 5, remembering that the latter are under natural ventilation. Time clips (i) and (iii), in which the surface temperature follows that of the mean thermal mass, have $\lambda \sim 1$, whereas time clips (iv) and (v), in which the surface temperature follows that of the interior air, have $\lambda \ll 1$. The smallest phase lag and attenuation between the mean thermal mass and interior air temperatures occur in time clips (iii) and (v), for which $\Omega_L < 1$, and the effective thermal mass is in good thermal contact with the interior air.

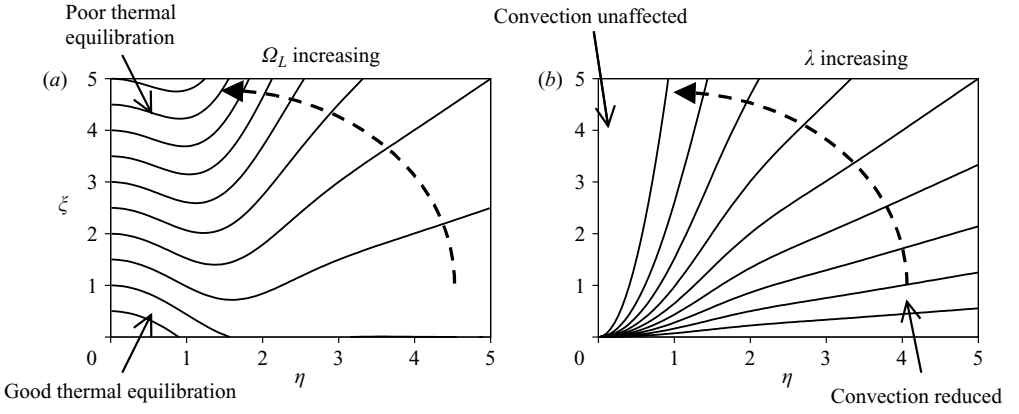

FIGURE 10. Contours of constant (*a*) $\Omega_L = 0.5, 1.0 \ldots 5.0$ and (*b*) $\lambda = 0.1, 0.2 \ldots 0.9$.

4. Approximate model of a naturally ventilated space with internal thermal mass

In the previous section we showed that if the interior air temperature variation is harmonic, the evolution of the internal thermal mass surface temperature is exactly replicated by that of a generalized lumped mass, with appropriate choice of parameters. We now explore whether a similar model can be applied to thermal mass influenced by a natural ventilation flow driving a nonlinear heat exchange between the environment, in which there is a harmonic temperature variation, and the interior air. As a starting point, we assume that the relationship between the thermal mass surface temperature and the mean thermal mass temperature in (3.5), that was the basis of the generalized lumped model, also holds under natural ventilation. This involves a degree of approximation because the nonlinearity introduced by natural ventilation causes the interior air (and thermal mass) temperatures to depart from a harmonic variation. In this model, the bulk thermal mass temperature evolves as

$$\Omega_L \frac{\mathrm{d}\theta_m}{\mathrm{d}\tau} = \theta_i - \theta_m, \tag{4.1}$$

(cf. 3.8), and the interior temperature is set by the requirement from (2.11) and (3.10) that the heat fluxes in the interior balance, i.e.

$$0 = \lambda(\theta_m - \theta_i) + F_n(\theta_e - \theta_i)|\theta_e - \theta_i|^{1/2}. \tag{4.2}$$

A numerical integration of (4.1) and (4.2) is again calculated for an initial-value problem, continuing until the long-time solution is reached. An adaptive step size Runge–Kutta algorithm is used for the time-stepping, with a simple interval bisection algorithm for determining θ_i; see Press *et al.* (1989). From (4.2), we see that the parameter F_n/λ is the appropriate measure of the relative importance of convective heat exchange at the surface of the thermal mass and the heat flux associated with the natural ventilation.

Figure 11(*a*) shows the interior air and thermal mass temperatures over several days, from numerical integration of the generalized lumped model, for parameters that correspond to the full diffusion calculation shown in figure 3. Visually the agreement with figure 3 is good (for comparison, the mean thermal mass temperature $l_r\theta_m$ is shown). A comparison of the phase lag and attenuation from the full model ($\times$) and the generalized lumped model ($\square$) for these thermal mass parameters is given

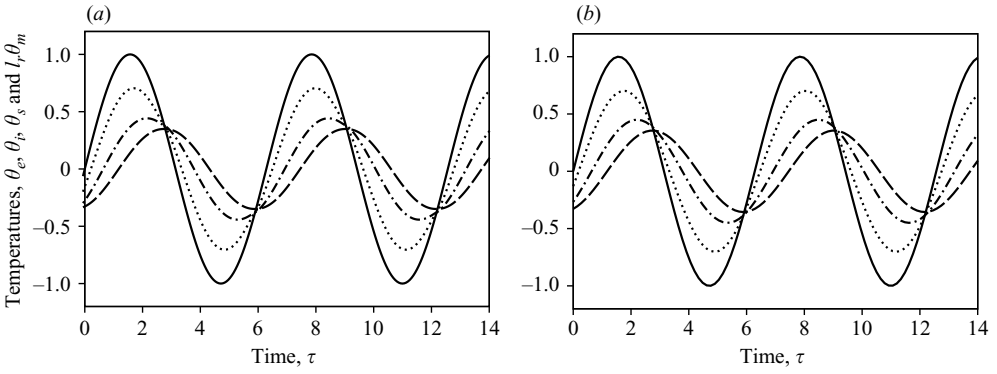

FIGURE 11. Timeseries of the temperature in the environment θ_e (solid), interior θ_i (dotted), thermal mass surface θ_s (dot-dashed) and mean thermal mass $l_r\theta_m$ (dashed), for $\Omega_L = 1.52$, $\lambda = 0.606$, $l_r = 0.921$ and $F_n = 2.0$, from (a) the generalized lumped model and (b) the approximate solution to this model found by the collocation method.

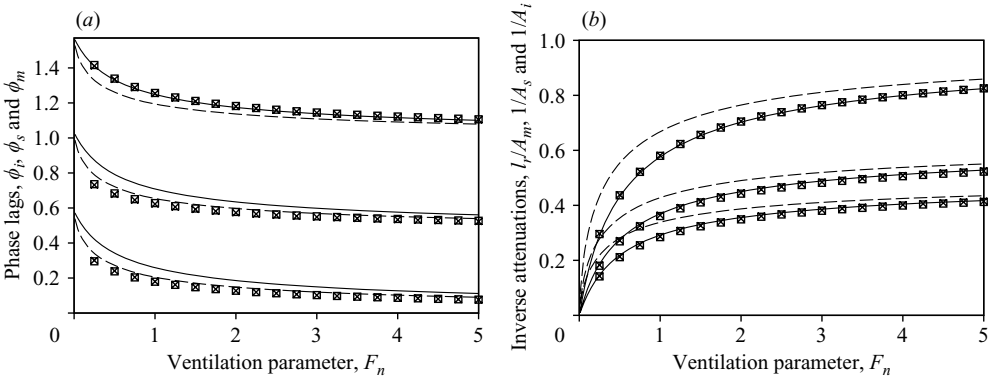

FIGURE 12. The variation in (a) phase lags and (b) attenuations from the full model ($\times$) with $\eta = 1$, $\xi = 1$, and the generalized lumped model ($\square$) with $\Omega_L = 1.52$, $\lambda = 0.606$, $l_r = 0.921$, both calculated numerically. Approximate solutions to the generalized lumped model found using the harmonic method (dashed lines) and the collocation method (solid lines) are shown.

in figure 12, across a range of ventilation rates. There is very good agreement over a wide range of values of F_n. This suggests that the generalized lumped mass model can be used as a good leading order model to describe the coupling of nonlinear natural ventilation with heat transfer into an internal thermal mass.

Although numerical integration of (4.1) and (4.2) is reasonably straightforward, considerable insight can be gained from approximate solutions of the coupled nonlinear system. This system can be reduced to a single nonlinear ordinary differential equation for θ_m,

$$\pm\left(\frac{\lambda\Omega_L}{F_n}\right)^{2/3}\left(\pm\frac{\mathrm{d}\theta_m}{\mathrm{d}\tau}\right)^{2/3} = \theta_e - \theta_m - \Omega_L\frac{\mathrm{d}\theta_m}{\mathrm{d}\tau}, \tag{4.3}$$

where the $\pm$ are taken together according to whether $\mathrm{d}\theta_m/D\tau \gtrless 0$. In the Appendix, we describe solutions of this equation that describe the transient cooling of a space with thermal mass towards a constant environment temperature, through natural ventilation.

An approximate solution to (4.3) can be found by the collocation method (method of selected points); see Zwillinger (1992). This is a weighted residual method, in which N unknown coefficients in a trial solution are determined from the requirement that the average residual errors in the differential equation, with N different weightings $\delta(\tau - \tau_{cj})$ for $j = 1, \ldots, N$, vanish over a suitable domain (here one period). This method has a long history, and when the basis functions for the approximation space are Fourier components, it forms the basis of the pseudospectral method. The choice of collocation points can affect the approximate solutions; see Collatz (1966). Here $\tau_{c1} = \phi_m$ and $\tau_{c2} = \phi_i$ are chosen to approximate the peak values. For the trial solution

$$\theta_m = \frac{\cos(\tau - \phi_m)}{A_m}, \tag{4.4}$$

the phase and attenuation of the thermal mass temperature are related by

$$A_m = \frac{1}{\cos \phi_m}, \tag{4.5}$$

so that, as in § 2, the bulk thermal mass, interior air and environment temperatures are equal at the thermal mass temperature extrema.The thermal mass phase lag varies with F_n/λ and Ω_L as

$$\left(\frac{\tan \phi_m}{\Omega_L} - 1\right)^6 = \left(\frac{\lambda^2}{\Omega_L F_n^2}\right)^2 \left(1 + \frac{1}{\Omega_L^2}\right)(1 + \tan^2 \phi_m). \tag{4.6}$$

A truncated series solution, calculated by the harmonic or spectral method, gives an alternative approximate solution to the collocation method. Taking the first term in the series, (4.4), as the trial solution, the orthogonality relationships reveal that the phase lag is

$$\frac{\tan \phi_m}{\Omega_L} = 1 + 1.07 \left(\frac{\lambda^2}{\Omega_L F_n^2}\right)^{1/3}. \tag{4.7}$$

While subsequent terms can be added to this series solution, increasing the accuracy, we have found that the prediction of the attenuation and phase lag is more accurate using the collocation method. Under either approximate method, from (4.1), the relative attenuation and phase lag of the thermal mass and interior air temperatures depend on Ω_L in the same manner as if the interior temperature were prescribed, as (3.16)–(3.17).

Figure 11(*b*) shows the interior air and thermal mass temperatures over several days, reconstructed from the approximate solution (3.16)–(3.19), (4.5) and (4.6), which is visually indistinguishable from the generalized lumped model solution in figure 11(*a*). The prediction of the phase lag and attenuation from the approximate solutions from the collocation method (solid lines) and from the harmonic method (dashed lines) are also shown in figure 12. The approximate solution found using the harmonic method gives a good estimate of ϕ_i and ϕ_s, but poor estimates of the other four indicators, while the approximate solution found using the collocation method is a good estimator of the numerical results for all but ϕ_i and ϕ_s.

A quantitative comparison of the full solution from (2.6), (2.7) and (2.11), the generalized lumped model solution from (4.1) and (4.2) and the approximate solution from (3.16), (3.17), (4.5) and (4.6) is now made. The square of the difference between the interior air and thermal mass surface temperatures from each of the latter two solutions, and temperatures θ_{i_exact} and θ_{s_exact} from the full model solution, is calculated over a day as a percentage of the squared variation of the environment

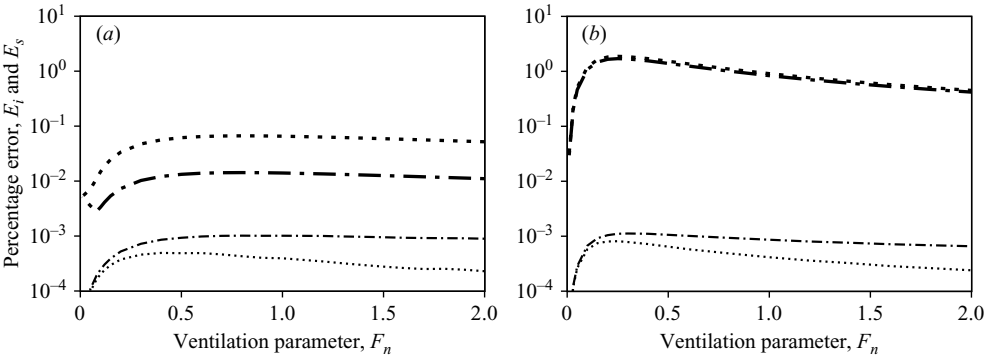

FIGURE 13. Percentage error in the temperature of the interior air E_i (dotted) and thermal mass surface E_s (dot-dashed), from both the generalized lumped model (thin curves) and the approximate solutions (thick curves) as compared with the full diffusion model. The parameters are (*a*) $\eta = 1$, $\xi = 1$, hence $\Omega_L = 1.52$ and $\lambda = 0.606$, and (*b*) $\eta = 0.5$, $\xi = 0.2$, hence $\Omega_L = 0.364$ and $\lambda = 0.546$.

temperature $\int_0^{2\pi} \theta_e^2 \, \mathrm{d}\tau = \pi$, i.e.

$$E_i = \frac{100}{\pi} \int_0^{2\pi} (\theta_i - \theta_{i\_exact})^2 \, \mathrm{d}\tau \quad \text{and} \quad E_s = \frac{100}{\pi} \int_0^{2\pi} (\theta_s - \theta_{s\_exact})^2 \, \mathrm{d}\tau. \tag{4.8}$$

The values of E_i and E_s for both the generalized lumped model, and the collocation method approximate solution, are shown in figure 13(*a*) for a range of ventilation parameters F_n, at $\eta = 1$, $\xi = 1$. For these parameters, the errors in solutions from the generalized lumped model are very small, and the errors in solutions from the collocation approximation, although somewhat greater, are less than 0.1%. In the generalized lumped model, for these values of η and ξ, and for all others for which $\Omega_L > 1$, E_i is greatest for an intermediate value of $F_n = O(\lambda)$, along the boundary between regimes I and III, while E_s reaches a plateau for large F_n. When $F_n \ll \lambda$, the temperature variations are small in both the full diffusion and generalized lumped models, while when $F_n \gg \lambda$, the interior temperature follows the (harmonic) environment temperature closely, and so the assumption on which the generalized lumped model is based is very good. The errors for the harmonic approximation (not shown) are many times greater than those for the collocation approximation. While the collocation approximation minimizes the error, the harmonic approximation minimizes the error at the fundamental frequency only, leading to a worse approximation at this level.

When the values of η and ξ are such that $\Omega_L \ll 1$, such as for the case of $\eta = 0.5$, $\xi = 0.2$ shown in figure 13(*b*), the errors E_i and E_s are greatest for $F_n = O(\xi)$, along the boundary between regimes I and II. From its definition, at $F_n \approx \xi$, ventilation brings in just enough heat during one forcing period to raise the temperature of the whole thermal mass, which behaves almost as a lumped mass for these small values of η. As the collocation points $\tau_{c1} = \phi_m$ and $\tau_{c2} = \phi_i$ are close together for these parameters, and the approximate solution is a bad estimator of the generalized lumped model behaviour.

With these points in mind, the variation in model errors across $\eta\xi$ parameter space is investigated, at the value of F_n that maximizes the error. The errors in the generalized lumped model solution are less than 0.1%. These errors are greatest for the thermal mass surface temperature at $\xi = O(1)$, along the boundary between

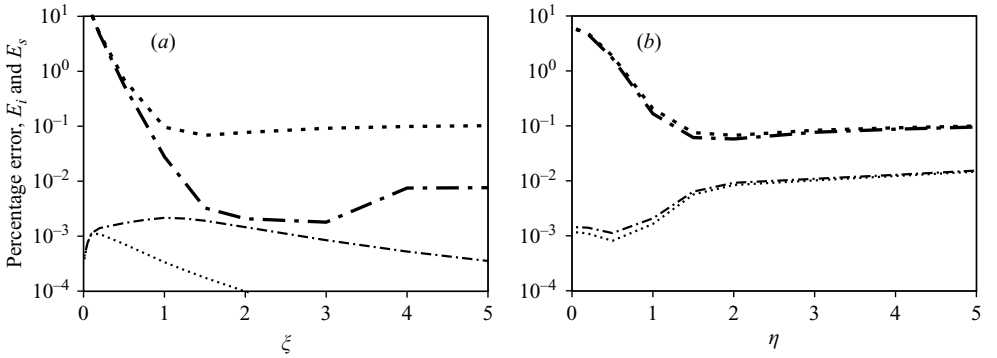

FIGURE 14. Maximum percentage error over F_n in the temperature of the interior air E_i (dotted) and thermal mass surface E_s (dot-dashed), from both the generalized lumped model (thin curves) and the approximate solutions (thick curves) as compared with the full diffusion model. The parameters are (*a*) $\eta = 0.2$ and (*b*) $\xi = 0.2$.

regimes II and III, as shown in figure 14(*a*), and increase by a factor of about 10 as η rises above 1, and the effective mass thickness is reduced below the actual thickness, as shown in figure 14(*b*). The errors in the theoretical approximation are less than 1% over most of the parameter space. These errors rise as $\xi \to 0$, as shown in figure 14(*a*), when again the collocation points $\tau_{c1} = \phi_m$ and $\tau_{c2} = \phi_i$ approach each other. The error is greater for small η, when a larger fraction of the thermal mass is affected by the temperature fluctuations at the surface, as shown in figure 14(*b*). For larger ξ, the error does not vary significantly with η.

With this confidence in the generalized lumped model and its approximate solution, we now explore the effects of internal thermal mass on the temperature evolution within the space. Three limiting forms of the solution to (4.6) can be derived.

Region I: $$\frac{F_n}{\lambda} \ll \min(1, \Omega_L)\left(1 + \frac{1}{\Omega_L^2}\right)^{1/4} \text{ (ventilation-limited),}\dagger$$

$$\tan\phi_m \sim A_m \sim \frac{\lambda\Omega_L}{F_n}\left(1 + \frac{1}{\Omega_L^2}\right)^{1/4} \gg 1, \quad A_i \sim \frac{\lambda}{F_n}\left(1 + \frac{1}{\Omega_L^2}\right)^{-1/4} \gg 1,$$

$$\tan\phi_i \sim \frac{\tan\phi_m}{1 + \Omega_L \tan\phi_m}.$$

Region II: $$\Omega_L \ll \min\left[1, \left(\frac{F_n}{\lambda}\right)^2\right] \text{ (convection-dominated),}$$

$$\tan\phi_m \sim \Omega_L + \left(\frac{\lambda^2\Omega_L}{F_n^2}\right)^{1/3} \ll 1, \quad A_m \sim A_i \sim 1 + \frac{\tan^2\phi_m}{2} \sim 1,$$

$$\tan\phi_i \sim \left(\frac{\lambda^2\Omega_L}{F_n^2}\right)^{2/3} \ll 1.$$

† In this regime, the interior/environment temperature difference scales on ΔT, and the non-dimensional time constant $\omega t_c = 1/\epsilon R_n = \Omega_L/F_n$ indicates the relative importance of heat storage by the thermal mass to heat transfer by ventilation. Hence the parameter combination Ω_L/F_n appears in the limiting form of the solution.

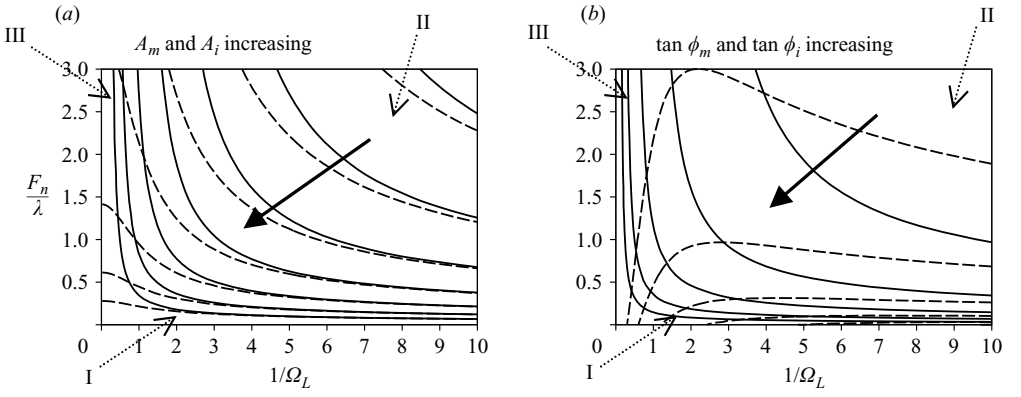

FIGURE 15. Contours of (*a*) attenuations A_m (solid lines) and A_i (dashed lines) at values 1.0625, 1.125, ..., 5.0 and (*b*) phase lags $\tan\phi_m$ (solid lines) and $\tan\phi_i$ (dashed lines) at values 0.3, 0.6, ..., 9.6, for the approximate solution from (4.6) to the generalized lumped model.

Region III: $\Omega_L \gg 1$, $\dfrac{F_n}{\lambda} \gg 1$ (interior air and thermal mass diverge),

$$\tan\phi_m \sim A_m \sim \Omega_L\left[1+\left(\frac{\lambda}{F_n}\right)^{2/3}\right] \gg 1, \quad A_i \sim 1+\left(\frac{\lambda}{F_n}\right)^{2/3} \sim 1,$$

$$\tan\phi_i \sim \frac{1}{\Omega_L}\left(\frac{\lambda}{F_n}\right)^{2/3} \ll 1.$$

There is a close correspondence between these regions and those in the scaling derived in § 2, with the asymptotes for the attenuation above providing greater detail, in addition to the new phase information. The parameter combination $\max(1,\eta)/\xi$ representing the degree of thermal equilibration between the effective thermal mass and the interior air is again equivalent to $1/\Omega_L$. The generalized lumped model shows that when convection can transfer heat to the thermal mass more quickly than diffusion can spread it within the thermal mass, the heat transfer coefficient is effectively reduced by the factor λ. Then the strength of the ventilation is characterized by F_n/λ, that is, the ratio of ventilation heat flux to the heat flux from the thermal mass at the reduced convection strength.

The variation of attenuation and phase lag with F_n/λ and Ω_L for the approximate solution is shown in figure 15. The attenuation of both the interior air and thermal mass temperature variations, and the phase lag of the thermal mass variation, increase with decreasing ventilation (F_n decreasing) and with decreasing heat exchange with the thermal mass (Ω_L increasing). The phase lag of the interior variations increases as F_n decreases, and peaks at a value of $\Omega_L = \Omega_{Lcrit} < 3^{-1/2}$ for any F_n, given by

$$\Omega_{Lcrit} = \sqrt{\frac{\sqrt{1+16\gamma}-(1+6\gamma)}{2(1-9\gamma)}} \quad \text{where} \quad \gamma = \left(\frac{F_n}{2\lambda}\right)^{4/3}. \tag{4.9}$$

This critical parameter value lies within regime I and between regimes II and III. At both extremes of Ω_L, the interior phase lag falls to zero. For close thermal equilibration between the effective thermal mass and the interior air ($\Omega_L \to 0$), the interior air and thermal mass temperatures both follow the environment, as there is no reservoir able

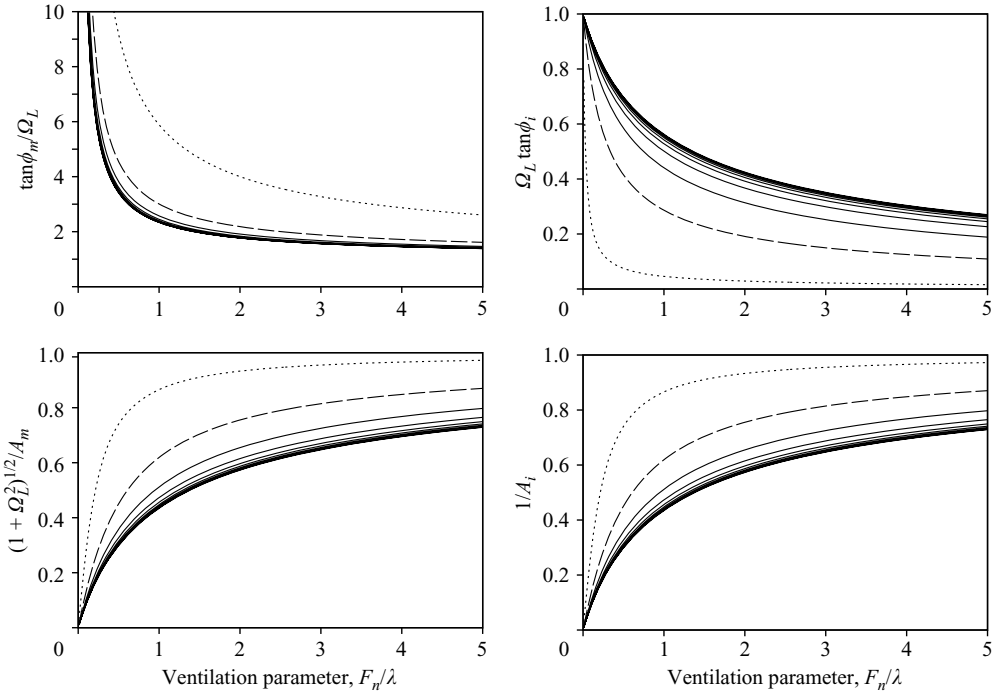

FIGURE 16. The variation with F_n/λ of the rescaled phase lags and attenuations from the approximate solution from (4.6) to the generalized lumped model, for $\Omega_L = 0.1$ (dotted line), 0.5 (dashed line) and 1.0, 1.5, ..., 5.0 (solid lines).

to maintain a different temperature. For little thermal equilibration ($\Omega_L \to \infty$), the interior temperature follows the environment, the interior having negligible thermal mass.

It is useful to know the ranges of the phase lags and attenuations. The interior phase lag is largest in the ventilation-limited regime, and from the scaling above therefore always satisfies $0 \leqslant \tan\phi_i \leqslant 1/\Omega_L$. The bulk thermal mass temperature always lags the interior temperature by Ω_L, and so $\Omega_L \leqslant \tan\phi_m < \infty$. As the ventilation parameter becomes large, the interior temperature follows the environment temperature, and so $1 \leqslant A_i < \infty$. The bulk thermal mass temperature is always attenuated below the interior air temperature by $\sqrt{1+\Omega_L^2}$, and so $\sqrt{1+\Omega_L^2} \leqslant A_m < \infty$.

A somewhat simplified scaling covers the range $\Omega_L \gg 1$, including the limits of regions I and III. Here, from (4.6), $\tan\phi_m \sim \Omega_L f(F_n/\lambda)$, where the function $f(x)$ satisfies

$$[f(x)-1]^3 \sim \frac{f(x)}{x^2}. \tag{4.10}$$

Since $f(x) > 1$, we then have the limiting forms $A_m \sim \Omega_L f(F_n/\lambda)$, $A_i \sim f(F_n/\lambda)$ and $\tan\phi_i \sim [1 - 1/f(F_n/\lambda)]/\Omega_L$. This collapse with F_n/λ at large Ω_L of the phase lags and attenuations, scaled by the limiting values, is shown in figure 16.

The success of the approximate solution to the generalized lumped model in capturing the behaviour of the full numerical model is confirmed in figure 17. The phase lag and attenuation of the interior air and mean thermal mass temperature for a number of choices of parameters (η, ξ, F_n) corresponding to three values of Ω_L

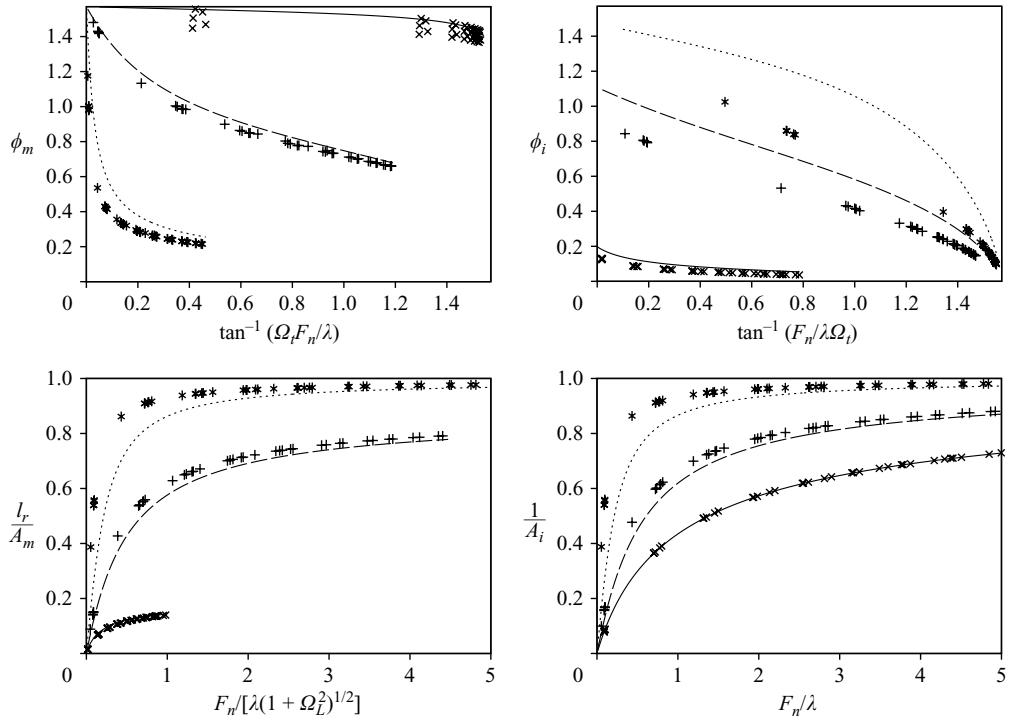

FIGURE 17. The phase lag and attenuation from numerical results of the full diffusion model (points) and from the approximate solution from (4.6) to the generalized lumped model (lines), with parameters chosen such that $\Omega_L = 0.1$ ($\star$ and dotted line, using $0.02 < \eta < 0.35$, $0.02 < \xi < 0.1$), $\Omega_L = 0.5$ ($+$ and dashed line, using $0.05 < \eta < 0.8$, $0.1 < \xi < 0.5$) and $\Omega_L = 5.0$ ($\times$ and solid line, using $0.1 < \eta < 5.0$, $5.0 < \xi < 20.0$). All results were calculated with $0 < F_n/\lambda < 5$.

are seen to collapse reasonably onto the approximate solution curves replotted from figure 16, dependent on (Ω_L, F_n/λ). Note once again that $A_{mean} = A_m/l_r$.

5. Conclusions

The air temperature inside a building depends on many factors, including the environment temperature, building geometry and heating. In buildings with significant thermal mass, the building fabric acts as a heat store, and the flux of heat between the fabric and air depends on the time history of temperature of the system. With modern construction techniques, the thermal mass in a building is typically insulated from the environment. While numerical integration of thermal diffusion within the thermal mass can give an exact solution, more insight and greater applicability in the design process can be gained from lumped models, in which the thermal mass has a uniform temperature.

An internal thermal mass under time-periodic forcing can be characterized by two parameters: the ratio ξ of the time for convection to affect the thermal mass temperature to the forcing time scale, and the ratio η of the layer depth to the penetration depth, through thermal conduction, of the varying signal. The evolution of the mean temperature of an internal thermal mass in contact with interior air at a harmonically varying temperature is reproduced exactly by a generalized lumped

mass model. In this model, heat is transferred from a lumped mass thinner by a factor l_r than the true thermal mass thickness, with convection at the surface weaker by a factor of λ than the true convection. It is equivalent to a resistor and capacitor in series to ground in the CTF method. The fraction l_r of the thermal mass which is in good thermal contact with the air increases with the penetration depth $1/\eta$ until the whole thickness of the thermal mass takes on a uniform temperature. When convection proceeds more rapidly than diffusion, heat builds up at the surface and convection is reduced by a factor λ, which decreases as ξ decreases and as η increases. The degree of thermal equilibration between the effective thermal mass and the interior air is then given by $1/\Omega_L$, where $\Omega_L = \xi l_r/\lambda$. The reduced convection is equivalent to introducing a surface temperature, between the bulk thermal mass and interior air temperature, which has an important influence on comfort conditions in the space.

The conditions inside a simple well-mixed single-space ventilated building have been investigated for a harmonically varying environment temperature. The internal thermal mass of the building is approximated with the generalized lumped model described above (although under natural stack ventilation, the ventilation heat flux varies nonlinearly with temperature difference and temperature variations are only approximately harmonic). The strength of the ventilation is quantified by the ratio F_n/λ of a typical ventilation heat flux to the heat exchange with the thermal mass under reduced convection. The bulk thermal mass temperature θ_m reaches its extrema when interior and thermal mass temperatures are all equal to the environment temperature, and so $A_m \cos\phi_m \approx 1$. The relative attenuation and phase lag of the thermal mass temperature from the interior temperature are the same as if the interior temperature was prescribed, so $(A_m/A_i)^2 \approx 1 + \Omega_L^2$ and $\tan(\phi_m - \phi_i) \approx \Omega_L$. When F_n/λ is small and ventilation is restricted, the interior air and bulk thermal mass temperatures vary by only a small amount, with the thermal mass phase lag almost $\pi/2$. When Ω_L is large and thermal equilibration between the thermal mass and interior air is poor, variations in the interior temperature are almost in phase with the environment and increase with F_n/λ, moving from the ventilation-limited regime to one in which the interior air temperature variations, although large, do not transfer significant heat to the thermal mass. Alternatively, when Ω_L is small, the variation in bulk thermal mass and interior air temperatures are similar and decrease in phase and attenuation as F_n/λ increases, moving from the ventilation-limited regime to one in which convection dominates.

Results from the generalized lumped model are very close to those from numerical integration of thermal diffusion within the thermal mass. An approximate solution to the generalized lumped mass model, found by the collocation method, also compares well with the numerical model, providing that ξ is not very small. This will not restrict the practical use of the model, since even lightweight building constructions are likely to fall outside this range. Therefore, estimates of the phase lag and attenuation of the interior, bulk and surface thermal mass temperatures can be gained from the approximate solution by three steps:

(i) estimate η, ξ and F_n for the space,

(ii) calculate the parameters Ω_L and λ for the generalized lump model,

(iii) solve (4.6) for ϕ_m, and calculate A_m, ϕ_i, A_i, ϕ_s and A_s from (4.5) and (3.16)–(3.19).

The neglect of internal thermal gains is the main simplification in this work, which will be addressed in a follow-up study. These investigations give an indication of the regimes that occur in naturally ventilated spaces with internal thermal mass. It would be of interest to determine the temperature variations within the space under the

more complex conditions of time-varying internal heat gains and ventilation opening areas.

In closing we note that the results of the present analysis of an insulated internal thermal mass are different from the case in which the thermal mass is in thermal contact with both the environment and interior air: in that case, the nonlinearity in the ventilation flow causes a sharp transition in regimes from a ventilation-controlled heat exchange to one controlled by the diffusive heat flux through the thermal mass, as the amount of thermal mass increases (Holford 2004). It would be interesting to combine the two models in a future analysis, to explore the interaction of both internal thermal mass, and thermal mass in good contact with the exterior as well as the interior. However, current building regulations require a sufficiently high degree of insulation for the building envelope that the penetration depths of interior and environmental temperature variations do not extend into more than a small fraction of the insulation. In this limit, it is anticipated that an external thermal mass supplies the same fluctuating heat flux as an internal mass with suitably chosen effective thickness, combined with a small steady heat flux through the imperfect insulation.

This work has been funded by the Cambridge MIT Institute, as part of research into low energy buildings.

Appendix. Transient ventilation of an internal thermal mass

A lumped model can also be used to represent the response of an internal thermal mass to a sudden change in environment temperature, in the limit $\eta \ll 1$, where here $\eta = l/\sqrt{2\kappa t}$, and t is the time elapsed since the sudden change, for which the signal of the change has diffused throughout the thermal mass. The adjustment of the thermal mass temperature with scaled time $\tau = \tau/\Omega_L = h\lambda t/\rho c l l_r$ to the environment $\theta_e = 0$ is then governed by

$$\mp\left(\frac{\lambda}{F_n}\right)^{2/3}\left(\pm\frac{\mathrm{d}\theta_m}{\mathrm{d}\tau}\right)^{2/3} = \theta_m + \frac{\mathrm{d}\theta_m}{\mathrm{d}\tau}. \tag{A 1}$$

Without loss of generality, taking the case $\theta_m(0) = 1$, and ignoring the invalidity of (A 1) for very small times, this becomes

$$0 = \theta_m - \left(\frac{\lambda}{F_n}\right)^{2/3}\left(-\frac{\mathrm{d}\theta_m}{\mathrm{d}\tau}\right)^{2/3} + \frac{\mathrm{d}\theta_m}{\mathrm{d}\tau}. \tag{A 2}$$

In the limit $F_n/\lambda \gg 1$, the ventilation is sufficient to provide no control on the heat transfer and the thermal mass temperature decays exponentially on the time scale $l_r t_2/\lambda$ for convection to affect the bulk thermal mass temperature,

$$\theta_m(\tau) = \mathrm{e}^{-\tau} = \exp\left(-\frac{\lambda}{l_r t_2}t\right). \tag{A 3}$$

In the limit $F_n/\lambda \ll 1$, convection is sufficient to provide no control on the heat transfer and the thermal mass temperature decays with a power law dependence on the time scale $2t_4 l_r/\epsilon$ for ventilation to affect the bulk thermal mass temperature,

$$\theta_m(\tau) = \left(1 + \frac{F_n\tau}{2\lambda}\right)^{-2} = \left(1 + \frac{\epsilon}{2t_4 l_r}t\right)^{-2}. \tag{A 4}$$

REFERENCES

Baines, W. D. & Turner, J. S. 1969 Turbulent buoyant convection from a source in a confined region. *J. Fluid Mech.* **37**, 51–80.

Bansal, N. K. & Bhandari, M. S. 1996 Comparison of the periodic solution method with TRNSYS and SUNCODE for thermal building simulation. *Solar Energy* **57**, 9–18.

Chartered Institution of Building Services Engineers 1999 *Environmental Design: CIBSE Guide A*. CIBSE, London.

Collatz, L. 1966 *The Numerical Treatment of Differential Equations*. Springer.

Cook, M. J., Lomas, K. J. & Eppel, H. 1999 Design and operating concept for an innovative naturally ventilated library. In *Engineering in the 21st Century: The Changing World*. In *Proc. CIBSE Nat. Conf.*, pp. 500–507. CIBSE, London.

Crisp, V. H. C., Fisk D. J. & Salvidge, A. C. 1984 *The BRE Low-Energy Office*. Department of the Environment, Building Research Establishment.

Department of Trade and Industry 2005 *Energy Consumption in the UK*. `http://www.dti.gov.uk/energy/inform/energy_consumption`.

Fisk, D. J. 1981 *Thermal Control of Buildings*. Applied Science.

Gebhart, B., Jaluria, Y., Mahajan, R. L. & Sammakia, B. 1988 *Buoyancy-Induced Flows and Transport*. Hemisphere.

Gladstone, C. & Woods, A. W. 2001 On buoyancy-driven natural ventilation of a room with a heated floor. *J. Fluid Mech.* **441**, 293–314.

Holford, J. M. 2004 Simple modelling of thermal mass. In *Proc. of RoomVent '04, 9th Intl Conf. on Air Distribution in Rooms* (ed. M. C. Gameiro da Silva). ADAI Universidade de Coimbra.

Holford, J. M. & Hunt, G. R. 2000 Multiple steady states in natural ventilation. In *Proc. 5th Intl Symp. on Stratified Flows* (ed. G. A. Lawrence, R. Pieters & N. Yonemitsu), pp. 661–666. University of British Columbia.

International Energy Agency 2005 *Key World Energy Statistics*. http://www.iea.org/dbtw-wpd/Textbase/nppdf/free/2005/key2005.pdf.

Kaye, N. B. & Hunt, G. R. 2004 Time-dependent flows in an emptying filling box. *J. Fluid Mech.* **520**, 135–156.

Li, Y. & Yam, J. C. W. 2004 Designing thermal mass in naturally ventilated buildings. *Intl J. Vent.* **2**, 313–324.

Linden, P. F., Lane-Serff, G. F. & Smeed, D. A. 1990 Emptying filling boxes: The fluid mechanics of natural ventilation. *J. Fluid Mech.* **212**, 300–335.

Lombard, C. & Mathews, E. H. 1999 A two-port envelope model for building heat transfer. *Build. Environ.* **34**, 19–30.

Long, K. 2001 Underneath the arches. *Building Design* 12 April 2001 15–17.

Mitalas, G. P. 1968 Calculation of transient heat flow through walls and roofs. *ASHRAE Trans.* **74**, 182–188.

Pratt, A. W. 1981 *Heat Transmission in Buildings*. Wiley.

Press, W. H., Flannery, B. P., Teukolsky, S. A. & Vetterling, W. T. 1989 *Numerical Recipes*. Cambridge University Press.

Rajapaksha, I., Nagai, H. & Okumiya, M. 2003 A ventilated courtyard as a passive cooling strategy in the warm humid tropics. *Renewable Energy* **28**, 1755–1778.

Stephenson, D. G. & Mitalas, G. P. 1967 Cooling load calculations by thermal response factors. *ASHRAE Trans.* **73**, III1.1–III1.7.

Yam, J., Li, Y. & Zheng, Z. 2003 Nonlinear coupling between thermal mass and natural ventilation in buildings. *Intl J. Heat Mass Trans.* **46**, 1251–1264.

Zwillinger, D. 1992 *Handbook of Differential Equations*. Academic.